Inventory of Supplementary Materials:

Figure S1, related to Figure 3: The LD binding domain of CCT1 alone is sufficient to fall off from shrinking LDs.

Figure S2, related to Figure 4: CCT1, but not GPAT4, CG9186 or LSD1, falls off shrinking water-in-oil drops.

Figure S3, related to Figure 5: Adding surfactant lipids does not affect CCT1 binding to the oil-water phase and highly compressed drops buckle their surface.

Figure S4, related to Figure 6: Proteins Compete for Binding at the Lipid Droplet Surface. LSD1 is predominantly LD-bound, independent of protein levels.

Figure S5, related to Figure 7: Duplication of the CCT M Domain Increases its Binding Affinity to the Lipid Droplet Surface.

References

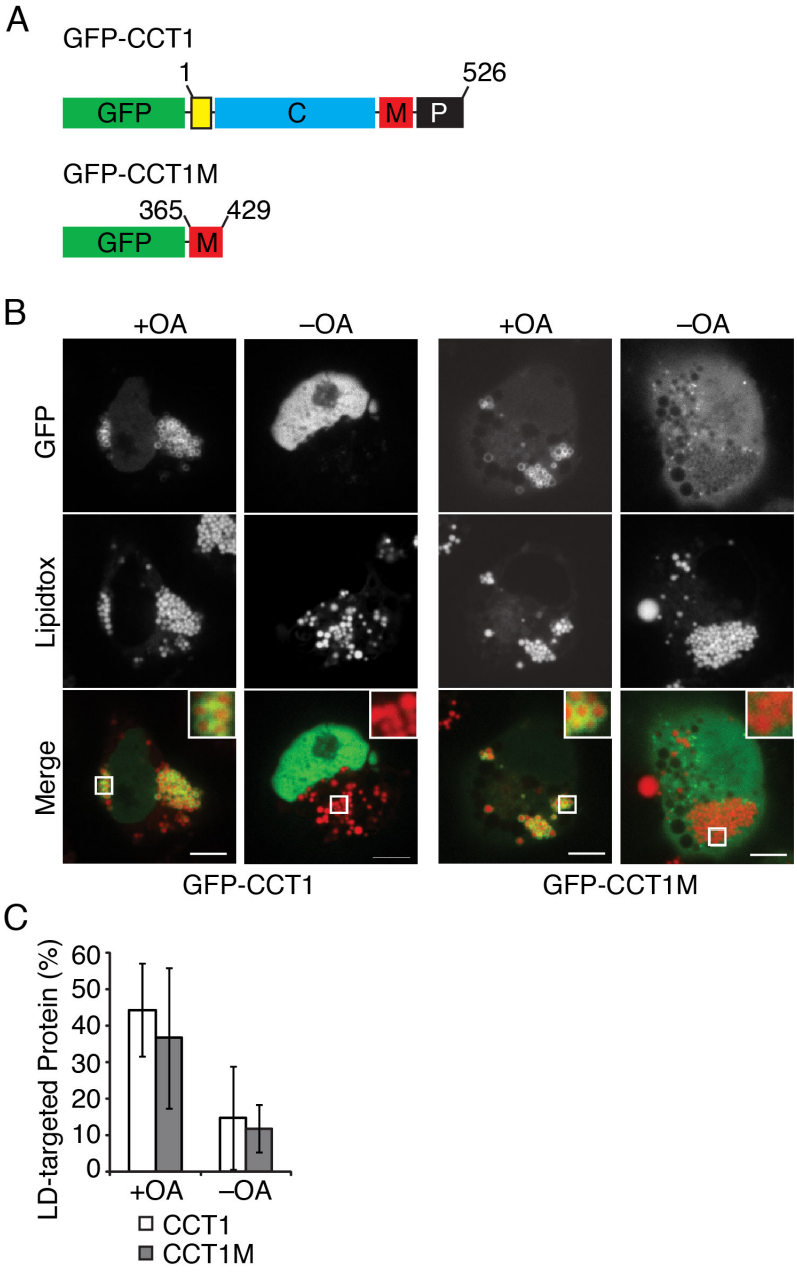

Figure S1, related to Figure 3: **The LD binding domain of CCT1 alone is sufficient to fall off from shrinking LDs.** (A) Schematic of full-length CCT1 and the CCT1 M-domain.

(B,C) The M-domain of CCT is sufficient to exhibit displacement from LDs. LDs were stained with LipidTOX. (B) Representative images are shown. Scale bar, 5 μm. Inlay, 3x magnification. (C) Mean fluorescence on LDs ± SD ($n > 15$). A.U. = arbitrary units.

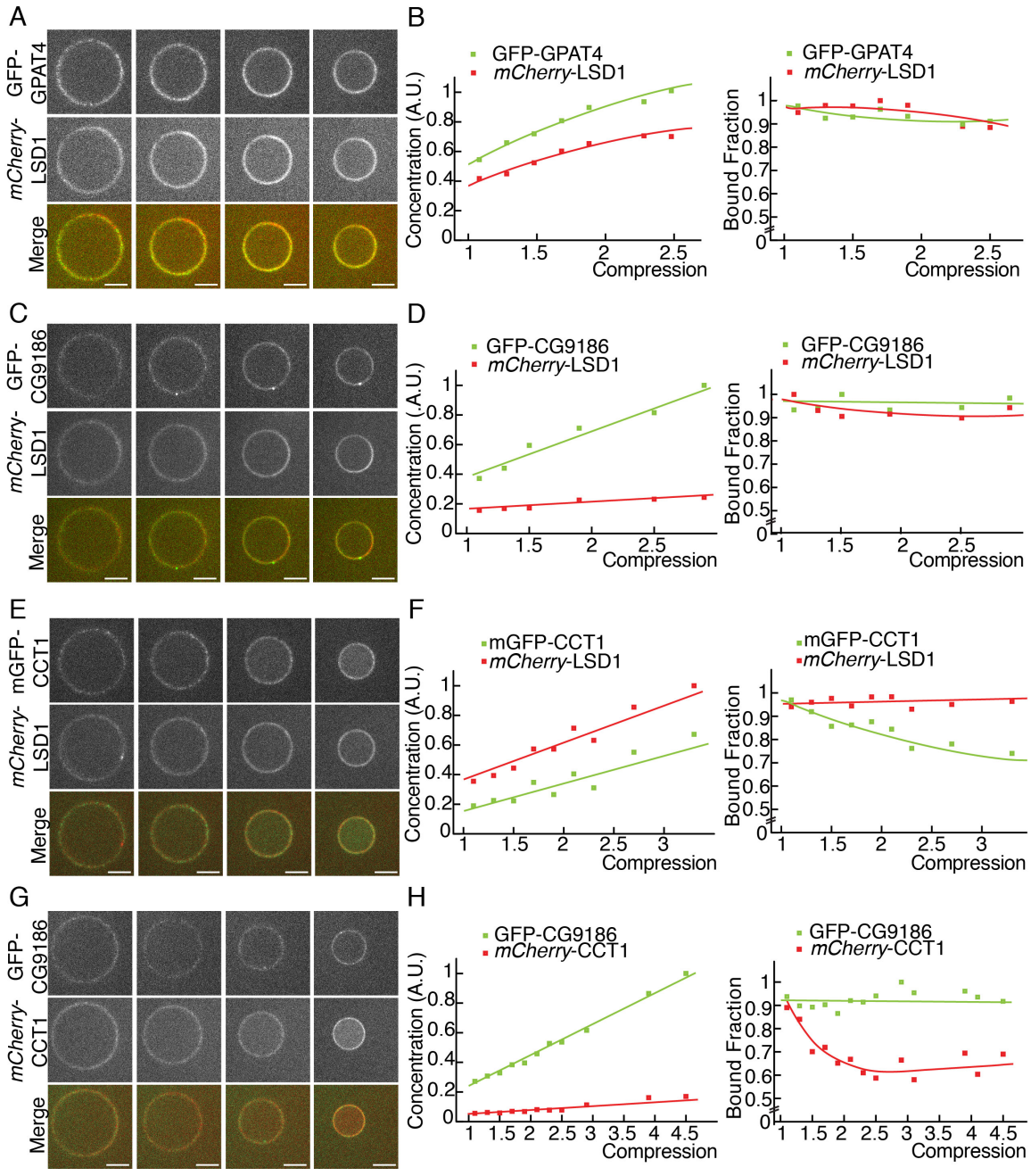

Figure S2, related to Figure 4: **CCT1, but not GPAT4, CG9186 or LSD1, falls off shrinking water-in-oil drops.** (A) LSD1 and GPAT4 remain bound during *in vitro* shrinkage of drops. Representative images are shown. Scale bar, 10 μm. (B) The levels of GFP-GPAT4 and mCherry-LSD1 on the surface increase during shrinkage. Surface mean concentration and mean surface-bound fraction for *mCherry*-LSD1 and GFP-GPAT4 are reported. Lines represent trends. A.U. = arbitrary units.

(C) LSD1 and CG9186 remain bound during in vitro shrinkage of drops. Representative images are shown. Scale bar, 10 μm.
(D) The levels of GFP-CG9186 on the surface increase during shrinkage. Surface mean concentration and mean surface-bound fraction for *mCherry*- LSD1 and GFP- CG9186 are reported. Lines represent trends. A.U. = arbitrary units.
(E) CCT1 is crowded out from the oil-water interface on drops containing LSD1. Representative images are shown. Scale bar, 10 μm.
(F) The levels of mCherry-LSD1 and mGFP-CCT1 on the surface increase during shrinkage. Surface mean concentration and mean surface-bound fraction for *mCherry*-LSD1 and mGFP-CCT1 are reported. Lines represent trends. A.U. = arbitrary units.
(G) CCT1 is crowded out from the oil-water interface on drops containing CG9186. Representative images are shown. Scale bar, 10 μm.
(H) The concentration of CG9186 on the surface increases during shrinkage. Representative images are shown. Scale bar, 10 μm. Values are means. Lines indicate trends. A.U. = arbitrary units.

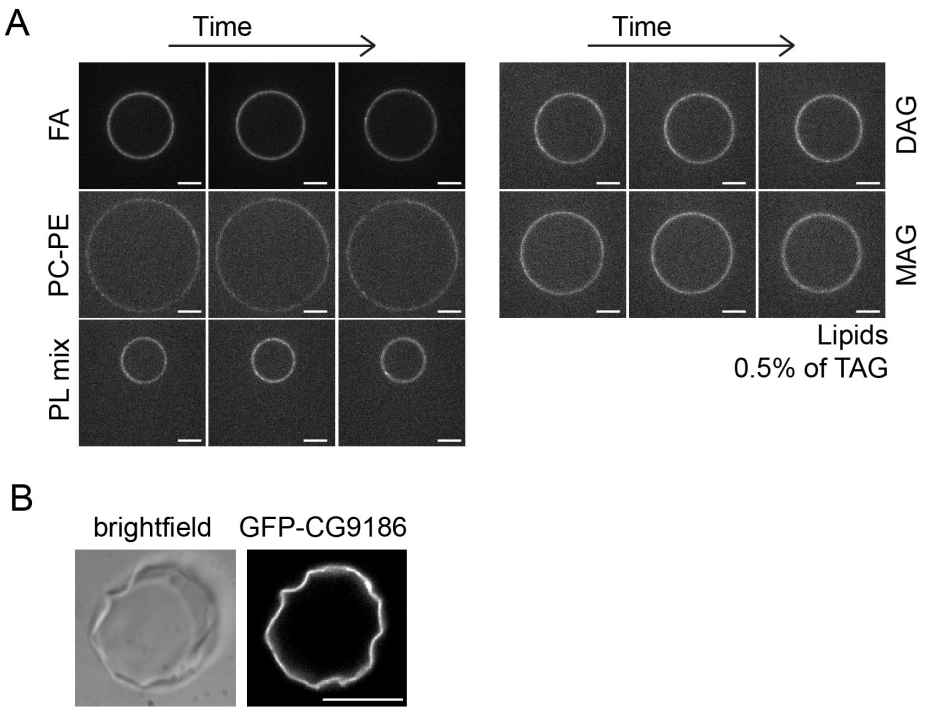

Figure S3, related to Figure 5: **Adding surfactant lipids does not affect CCT1 binding to the oil-water phase and highly compressed drops buckle their surface.** (A) Changes in lipid composition do not affect localization of CCT on drops *in vitro* during shrinkage. Lipids tested included oleic acid (FA), dioleoyl glycerol (DAG), monooleoyl glycerol (MAG), mixtures of phosphatidylethanol-amine (PE) and phosphatidylcholine PC (0-100, 50-50, 100-0), a phospholipid mixture mimicking LDs phospholipid composition (Thiam et al., 2013). Representative images are shown. Time > 1 hr. Scale bar, 10 μm. (B) At extreme compression, the high protein density on water-in-oil drops leads to surface buckling. Drop contained GFP-CG9186 bound to the surface. A representative image is shown. Scale bar, 10 μm.

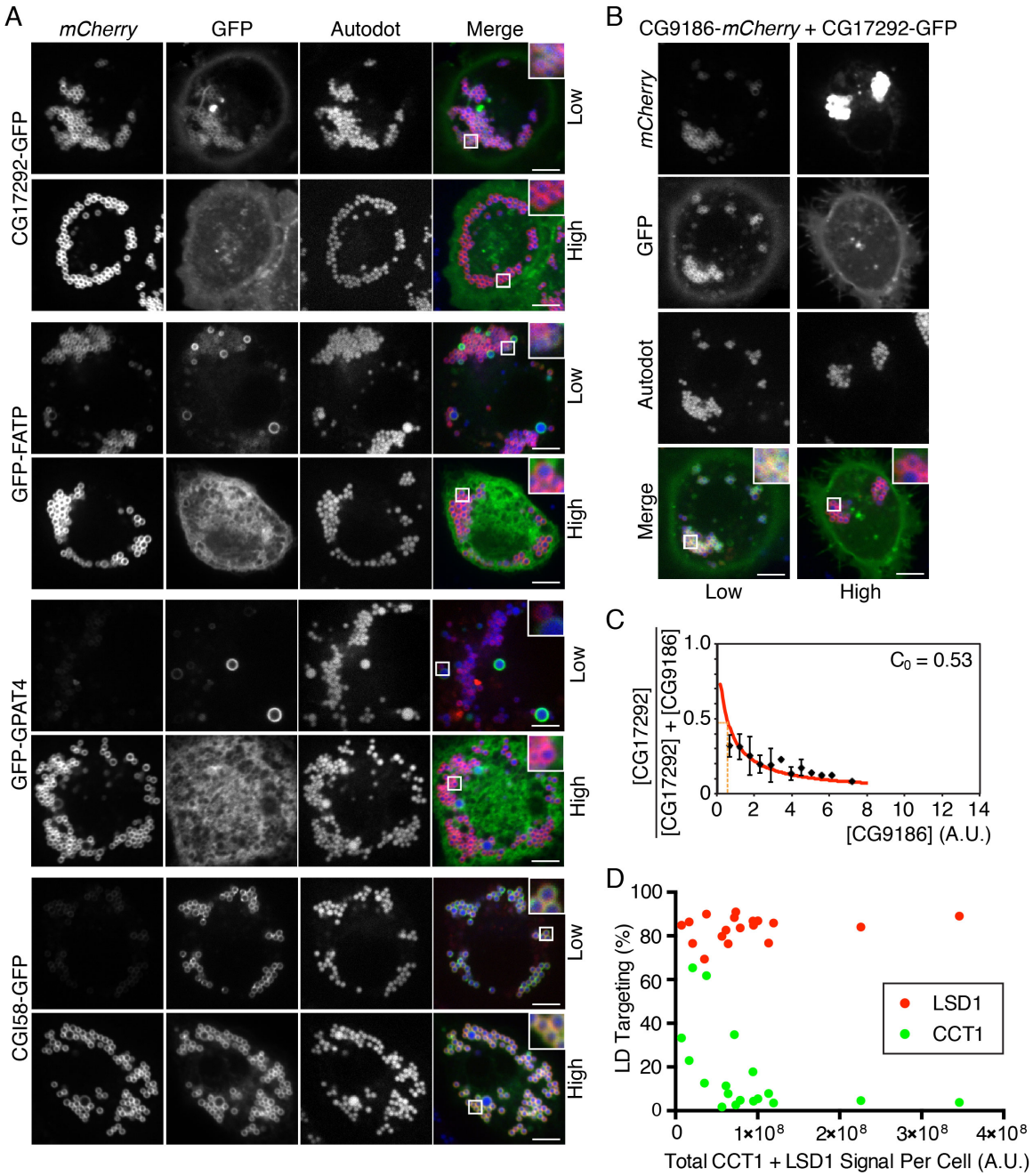

Figure S4, related to Figure 6: **Proteins Compete for Binding at the Lipid Droplet Surface. LSD1 is predominantly LD-bound, independent of protein levels.**

(A) Increased levels of LSD1 resulted in decreased levels of most GFP-tagged proteins on the surface of LDs. *mCherry*-LSD1 was co-expressed with GFP-CCT1 in LD-containing Drosophila S2 cells. For each protein combination, one representative cell with low expression (upper panels) and one with high

expression of LSD1 (lower panels) are shown. LDs were stained with AUTOdot. Representative images are shown. Scale bar, 5 μm. Inlay, 3x magnification.
(B,C) CG9186 outcompetes CG17292 at the lipid droplet surface. One cell with low expression (left panel) and one with high expression of CG9186 (right panel) are shown. LDs were stained with AUTOdot. (B) Representative images are shown. Scale bar, 5 μm. Inlay, 3x magnification. (C) Quantification. C_0 is the concentration of CG9186 needed to displace CG17292 form LDs. A.U. = arbitrary units. (D) Despite increased levels of other GFP-tagged LD proteins, LSD1 remains predominantly (~80%) bound. % LD-targeting of LSD1 and CCT1 was measured in cells and plotted against the total signal of fluorescent proteins in the same cells.

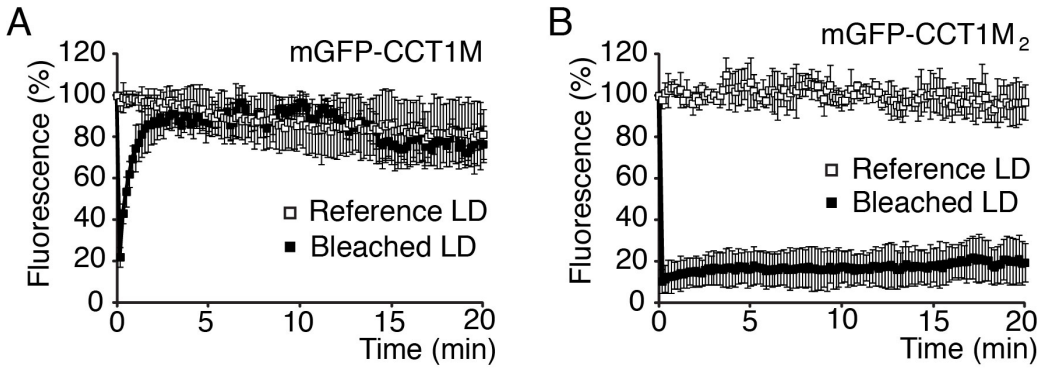

Figure S5, related to Figure 7: **Duplication of the CCT M Domain Increases its Binding Affinity to the Lipid Droplet Surface.** One M-domain (A) has a higher on-rate than a construct containing two copies of the M domain (B) according to FRAP analysis. At time 0 min, one LD per cell was photobleached. For mGFP-CCT1M and mGFP-CCT1M$_2$ the normalized fluorescence intensities of the bleached LD (black solid squares) or of an unbleached reference LD in the same cell (empty squares) are shown over time. Values are means ±SD of three experiments. Apparent on-rate of mGFP-CCT1M$_2$ is 0.047/min versus 1.13/min for mGFP-CCT1M.

References

Thiam, A.R., Antonny, B., Wang, J., Delacotte, J., Wilfling, F., Walther, T.C., Beck, R., Rothman, J.E., and Pincet, F. (2013). COPI buds 60-nm lipid droplets from reconstituted water-phospholipid-triacylglyceride interfaces, suggesting a tension clamp function. Proceedings of the National Academy of Sciences of the United States of America *110*, 13244-13249.